

## DIRECT EXPERIMENTAL EVIDENCE OF ELECTROMAGNETIC INERTIA MANIPULATION THRUSTING

Hector H. Brito

*Senior Member AIAA, Instituto Universitario Aeronautico  
Ruta 20, Km. 5.5, X5010JMN, Córdoba, Argentina*

Sergio A. Elaskar

*Fac. de Ciencias Exactas, Fís. y Nat., Universidad Nacional de Córdoba  
Av. Velez Sarsfield 1601, 5000 Córdoba, Argentina*

### ABSTRACT

New experimental results suggesting that “propellant-less” propulsion without external assistance is being achieved by means of electromagnetic (EM) inertia manipulation, are discussed here and compared with previous work along the same line of research. The underlying theory, based on Minkowski’s Energy-Momentum tensor for describing field-matter interactions, together with an alternative mass tensor formulation, both justifying that the inertial properties of the field generating device can be modified, are revisited. Former tests of an electromagnetic inertia manipulation thruster, engineered up to the “proof of concept” level, having yielded increasingly sharper and clearer evidence of alternate, then sustained thrusting, are briefly discussed. Recent testing activities, where increased power, improved power processing strategy and optimal use of the sensing device sensitivity were applied, resulted in a direct thrust signal, as observable in time domain plots. These results, on the basis of a reassessment of uncertainties, are shown to be consistent with an alternative formulation of Minkowski’s EM force density, which correctly predicts former peer-reviewed experimental results. They remain meanwhile controversial since the system momentum is not conserved. A conjectural approach based on the mass tensor concept allows for a tentative explanation, its predictions showing a complete agreement with the new experimental data.

### INTRODUCTION

Either to go to the stars or, more pragmatically, to substantially cut down space transportation costs, new propulsion mechanisms must be found which get rid of propellants and/or conventional external assistance, i.e., the mythical “space drive” must still be invented.<sup>1</sup>

Recent theoretical works show that jetless-sailless-beamless-tetherless propulsion can be achieved by manipulating the spaceship inertia in a way analogous to a dancer who increases her angular velocity by manipulating her body moment of inertia. The analogy goes this way: By considering space-time instead of 3-space, the spaceship 4-velocity (angular velocity analog) can be changed by manipulating its mass tensor components (moment of inertia tensor analog). To do that, an “extended” spaceship including the fields it eventually generates must be considered; a thrust then appears on the “material” spaceship by means of momentum exchange with its “field” counterpart. It follows from this picture that the 4-Momentum of the system should be conserved. The whole concept is embodied in the Covariant Propulsion Principle (CPP) which derives from a relativistic covariant mass tensor description of the closed system consisting of the rocket driven spaceship and its propellant mass, provided the “solidification” point is other than the system center of mass.<sup>2</sup>

When the EM field is chosen as the “field” counterpart, one may wonder if a static EM momentum can develop in the rest frame of the “material” spaceship. A possibility arises from a physical arrangement of electric and magnetic sources including polarizable media, as depicted in Fig. 1. Different theoretical results are possible depending whether Planck’s principle of inertia of the energy is satisfied or not between the Poynting vector (energy flow density) and the EM momentum density.<sup>3</sup> The results are basically Abraham’s and Minkowski’s forms of the EM momentum density, three dimensional expressions of the so called “Abraham-Minkowski controversy” about the correct Energy-Momentum tensor of EM fields in polarizable media. The controversy, lasting since 1909, strikingly remains as a yet unsolved issue of Physics,<sup>4,5</sup> with existing experimental evidence not allowing yet to draw definite conclusions.

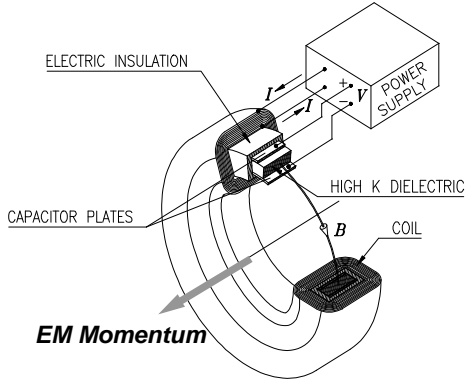


**Fig. 1** Stationary regime in the ‘matter’ rest frame with polarized media (Electromagnetic Momentum Generator).

By Minkowski’s formalism, a non-vanishing momentum of electromagnetic origin is shown to arise for the particular device depicted in Fig. 1.<sup>6-8</sup> It follows that the EM field can modify the inertial properties of the generating device, their variation producing forces on the device without any exchange of mass-energy with the surrounding medium. A propulsion concept based upon this kind of inertia manipulation mechanism was subsequently drawn; an electromagnetic inertia manipulation (EMIM) thruster was engineered up to the “proof of concept” level and experiments were designed and performed yielding by spectral analysis techniques, in an exploratory phase, indirect evidence of Minkowski’s approach being valid. In a second phase, with a slightly modified experiment, sharper and clearer evidence of sustained thrust has been found, as observed in frequency domain plots, too.<sup>9-11</sup> However, this sustained thrust must be considered a kind of “anomalous” effect since the Law of Momentum Conservation seems to be violated. This paper aims at presenting additional experimental work, where direct evidence of EMIM sustained thrust seems to emerge from the obtained results, as compared with theoretical predictions.

## **THEORETICAL BACKGROUND**

### **The EM Field Momentum Approach**

The device depicted in Fig. 1 bears an EM momentum density distribution in its rest “matter” frame, i.e., in the frame collocal with the hardware when all EM fields are off. This comes directly out from the particular electric and magnetic fields distribution, namely “crossed” fields, which enter the following mathematical expression of the EM momentum density:

$$\text{Abraham's claim: } \mathbf{g}^A = \frac{(\mathbf{E} \times \mathbf{H})}{c_0^2}, \quad (1)$$

$$\text{Minkowski's claim: } \mathbf{g}^M = (\mathbf{D} \times \mathbf{B}). \quad (2)$$

Abraham’s expression is fully consistent with Planck’s principle of inertia, since  $\mathbf{E} \times \mathbf{H}$  represents the EM energy flow, whereas Minkowski’s is not. Eqs. (1,2) are the vector expressions of the still-standing Abraham-Minkowski controversy about the form of the electromagnetic Energy-Momentum tensor, especially for low frequency or quasi-stationary fields.<sup>3,12-14</sup> The question arises whether these non-zero EM momentum densities can lead to a non-zero total EM momentum. It has been shown for any closed matter-field configuration that, provided the fields die out rapidly at infinity,<sup>15</sup> the total EM momentum in the “matter” rest frame can generally be written as:

$$\mathbf{G}^{(f)} = \int_V \mathbf{g}^{(f)} dV = \int_V \frac{\mathbf{x}}{c_0^2} \left[ \frac{\partial w}{\partial t} - \text{grad} \left( \frac{c_0}{c_F} \right)^2 \cdot \mathbf{s}^{(f)} - \left( \frac{c_0^2}{c_F^2} - 1 \right) \text{div} \mathbf{s}^{(f)} \right] dV, \quad (3)$$

where  $\mathbf{g}^{(f)}$  represent the EM field momentum density,  $\mathbf{s}^{(f)}$  is the EM energy flow;  $w$  is the total energy density;  $\mathbf{x}$  is the position vector;  $c_0$  is the velocity of light in vacuum and  $c_F = c_0$  in Abraham’s formulation, whereas  $c_F = c$ , velocity of light in the medium, in Minkowski’s formulation. For stationary regimes Eq. (3) writes:

$$\mathbf{G}^{(f)} = \int_V \mathbf{g}^{(f)} dV = - \int_V \mathbf{x} \left[ \text{grad} \left( \frac{1}{c_F^2} \right) \cdot \mathbf{s}^{(f)} + \left( \frac{1}{c_F^2} \right) \text{div} \mathbf{s}^{(f)} \right] dV \quad (4)$$

The quantity between brackets being  $\text{div} \mathbf{g}^{(f)}$ , a non-zero LHS is possible provided  $\mathbf{g}^{(f)}$  is not divergence-free everywhere. This can be achieved for arbitrary matter-field configurations if gradients of the velocity of light occur in the region of integration, i.e., if Minkowski’s formulation is adopted. This is the case for the setup shown in Fig. 2, where  $\text{div} \mathbf{s}^{(f)} = 0$  everywhere and a non-vanishing total EM momentum can only arise from the RHS first term of Eq. (4). The contributions for the volume integral come from the free surfaces of the dielectric, through which jumps of the velocity of light hold in the direction of the EM energy flux.

For this particular setup, transient regimes do not allow to produce an EM momentum contribution, since the

energy density variation rates distribute symmetrically throughout the setup regions.

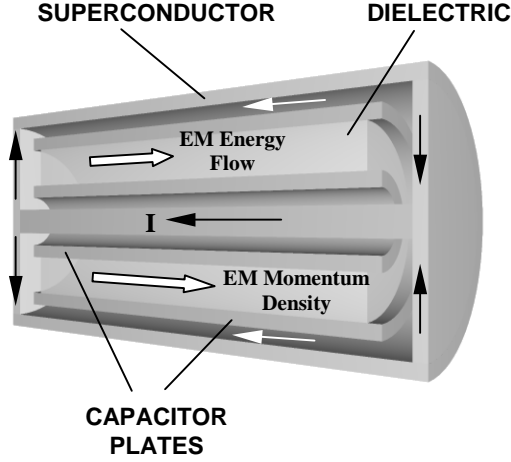


**Fig. 2** Stationary regime in the ‘matter’ rest frame with polarizable media.

Since for closed systems the Law of Momentum Conservation implies:

$$\int_V (\mathbf{g}^{(m)} + \mathbf{g}^{(f)}) dV = \text{const.}, \quad (5)$$

it follows

$$\frac{D}{Dt} \int_V \mathbf{g}^{(m)} dV = - \frac{D}{Dt} \int_V \mathbf{g}^{(f)} dV, \quad (6)$$

where  $D/Dt$  stands for material derivative w.r.t. time of the volume integral. Therefore, the LHS of Eq. (6) is the total force acting upon the system matter, i.e., the **thrust**. As previously seen, this thrust can amount to something different from zero provided Minkowski’s expression for the EM momentum density is applied. As for the RHS of Eq. (6), it can generally be expressed as (Transport Reynold’s Theorem):

$$\frac{D}{Dt} \int_V \mathbf{g}^{(f)} dV = \int_V \left[ \frac{\partial \mathbf{g}^{(f)}}{\partial t} + \text{div} (\mathbf{g}^{(f)} \mathbf{v}) \right] dV. \quad (7)$$

Since for stationary regimes non-zero total EM momentum can only occur in material domains, the following general expression for the electromagnetic thrust on closed systems can be derived

$$\mathbf{T} = - \int_{V_m} \frac{\partial \mathbf{g}^{(f)}}{\partial t} dV - \int_{\partial V_m} \mathbf{g}^{(f)} \mathbf{v} \cdot \mathbf{n} dS. \quad (8)$$

Assuming incompressible media and uniform velocity fields, Eq. (8) becomes

$$\mathbf{T} = - \int_{V_m} \frac{\partial \mathbf{g}^{(f)}}{\partial t} dV - \mathbf{v} \cdot \int_{\partial V_m} \mathbf{g}^{(f)} \mathbf{n} dS. \quad (9)$$

When applying Eq. (9) to the device depicted in Fig.1, it can be seen that, for quasi-stationary regimes, the EM momentum densities are negligible outside the material boundaries (besides a tiny radiation field). The RHS of Eq. (9) practically reduces to the first term. This is strictly true when the device is at rest in the observer’s frame. For practical purposes

$$\mathbf{T} \cong - \int_{V_m} \frac{\partial \mathbf{g}^{(f)}}{\partial t} dV = - \int_{V_m} \frac{\partial}{\partial t} (\mathbf{D} \times \mathbf{B}) dV. \quad (10)$$

According to Eq. (10), EM inertia manipulation becomes a theoretical possibility. A positive answer concerning Minkowski’s formulation would thus allow for “jet-less” propulsive effects by means of EM fields manipulation.

### The Mass Tensor Approach

It is always possible to represent the Electromagnetic Momentum Generator (EMMG) as a single particle located at the “matter” system c.o.m. (or any “structural” point). When the ON condition is set, the whole system must include the EM fields being created under such a condition, so that according to Ref. 2 a mass tensor is readily found as related to the whole system, such as, assuming closed system, in geometric notation

$$d(\mathbf{M} \cdot \mathbf{v}) = \mathbf{0}, \quad (11)$$

with

$$\mathbf{M} = (m_0 + m_{EM}^*) \mathbf{I} + (\mathbf{p}_{EM} \wedge \mathbf{v}) / c_0^2, \quad (12)$$

where  $m_0$  and  $m_{EM}^*$  represent the masses of the spaceship and the EM fields, respectively, in the spaceship rest frame;  $\mathbf{I}$  is the identity 4-tensor;  $\mathbf{p}_{EM}$  the 4-momentum of the EM field and  $\mathbf{v}$  the 4-velocity of the “solidification point”. From Eqs. (11) and (12) the 4-thrust on the single particle, in any arbitrary frame, is found to be given by

$$\mathbf{T} = - \frac{d \mathbf{p}_{EM}}{d \tau}, \quad (13)$$

which projects into 3-space as

$$\mathbf{T} = - \frac{d \mathbf{p}_{EM}}{d t}. \quad (14)$$

Keeping in mind that  $\mathbf{p}_{EM} \equiv \mathbf{g}^{(f)}$ , both Eqs. (6) and (14) expresses the same concept; different derivatives notation arise because the physical property on which they operate ascribes to an extended system in one case, and to a point mass in the other case. Equation (14) expresses, as expected, the law of conservation of the total system energy-momentum, consistently with Eq. (11). The change of the mechanical momentum exactly balances the change of the EM field momentum; momentum is then being exchanged within the whole closed system. The device works as an EM field momentum “accumulator” whereas the mechanical momentum that can be drawn from is, by present Physics paradigms, limited to the EM field momentum amount.

However, an unpublished conjectural approach based on the mass tensor concept suggests that the “accumulator” limitation can be circumvented. Two conjectures are enounced: 1) Mass/Inertia can acquire a tensor nature – 2) Translational motion in gravity-free regions is not affected by tensor mass rotations (like systems rotating around their c.o.m.).<sup>16,17</sup> The First Conjecture has been proved in Ref. 2, the Second Conjecture plainly states that Eq. (14) is no longer valid when the EM momentum changes derive from rotations in 3-space of the EM momentum carriers. This translates into a modified equation of motion, as follows

$$d(\mathbf{M} \cdot \mathbf{v}) = d^R \mathbf{M} \cdot \mathbf{v} , \quad (15)$$

where  $d^R \mathbf{M}$  represents the tensor mass variation due to rotations in 3-space of the EM momentum carriers. The 4-thrust definition is accordingly modified as

$$\mathbf{T} = - \frac{d \mathbf{p}_{EM}}{d \tau} + \frac{d^R \mathbf{p}_{EM}}{d \tau} . \quad (16)$$

Thrust in 3-space comes readily out from the 4-thrust spacelike components, being given by

$$\mathbf{T} = - \frac{d^{**} \mathbf{p}_{EM}}{d t} , \quad (17)$$

where  $(\cdot)^{**}$  stands for derivation w.r.t. time in the instantaneous rotating frame of the system. Thrust is, according to the 2<sup>nd</sup> Conjecture, related to the intrinsic variation of the EM momentum, as measured in the generating device comoving frame. By Eqs. (15) conservation of the system 4-momentum no longer holds and, in order to preserve the general validity of the law of energy-momentum conservation, one must admit that the system cannot be any longer considered as a closed one.

### The EM Force Density Approach

There is an another variant of the Abraham-Minkowski controversy, this time in terms of force densities. If dispersion is negligible and the medium is allowed to be isotropic but spatially inhomogeneous,  $\mathbf{D} = \epsilon \mathbf{E}$ ,  $\mathbf{B} = \mu \mathbf{H}$ . The force densities are given by<sup>3,10</sup>

$$\mathbf{f}^M = \rho \mathbf{E} + \mathbf{j} \times \mathbf{B} - \frac{1}{2} E^2 \nabla \epsilon - \frac{1}{2} H^2 \nabla \mu , \quad (18)$$

$$\mathbf{f}^A = \mathbf{f}^M + \frac{\epsilon_r \mu_r - 1}{c_0^2} \frac{\partial}{\partial t} (\mathbf{E} \times \mathbf{H}) . \quad (19)$$

These force densities clearly differ inside matter for generic fields; they are identical for static fields, irrespective of the medium. If harmonic fields are considered, the force densities instantaneous values differ but their averaged values become identical and therefore useless for discriminating between the two formulations. This is the reason Walker&Walker’s claim,<sup>18</sup> favoring Abraham’s one, is essentially wrong and their experiment remain inconclusive.

When application is made to the device of Fig. 1, with both  $\mathbf{D}$  and  $\mathbf{B}$  fields subjected to harmonic evolution, Eq. (18) can be used for its theoretical estimation, with the assumption that the polarization current in the dielectric contributes to the second term of the equation. As a result, the following expression for the EM average thrust on a closed system, as a function of the harmonic voltage  $V \sin \omega t$  on the width  $d$  capacitor and the harmonic current  $I \sin(\omega t + \phi)$  on the  $n$  turns coil, is found<sup>10</sup>

$$\langle F \rangle = \frac{\epsilon_r \omega n I V d}{2 c_0^2} \sin \phi . \quad (20)$$

The results obtained with Walker&Walker’s experiments are consistent with this formulation and can, as the authors did, be interpreted in terms of the polarization current contribution to the Lorentz force. However, Eq. (20) must be seen as a conflicting result if total momentum is conserved. In fact, the standard treatment of the problem requires the polarization current to be excluded from the magnetic contribution to the Lorentz force, so the averaged value cancels out. On the other hand, Eq. (20) is found to be consistent with Eq. (17) as applied to the EM momentum carriers in polar dielectrics. Therefore, thrust experiment involving harmonic fields in a closed system should allow to discriminate between the “standard” and the “proposed” formulation.

## **SUSTAINED THRUST EXPERIMENTS - 1**

Description and results of experiments geared to obtain sustained (or “rectified”) EMIM propulsive effects, were previously detailed elsewhere.<sup>9-11</sup> A summary of the relevant aspects is reproduced here for better understanding of new operating procedures and the resulting experimental data.

### **Experimental Setup Rationale**

The experimental setup basically consists of mounting the device as a seismic mass atop a thin vertical cantilever beam (a resonant blade), sitting on a vibration-free platform. Piezoceramic strain transducers (PZTs) are used to detect the seismic mass displacements through output voltages proportional to the strain level in a broad dynamic range, achieving sensitivities up to  $10^{-11}$  m/m.<sup>19</sup> The transducer analog output signal is digitalized for further processing through a 12 Bit data acquisition board, making it available to PC based storage devices. Sustained thrust experiments were implemented in order to get rid of previously observed interfering effects considered potential sources of uncertainties.

By applying power to the EMMG so that  $D$  and  $B$  fields were subjected to harmonic evolution with variable phase shift, a non-zero averaged (sustained) thrust was sought after in virtue of Eq. (20). To take advantage of the sensing device characteristics, the voltage supply is reversed at a frequency different from the AC supply frequency, so the seismic setup is set into vibratory motion if the “proposed” formulation is correct. By detecting this force, the geomagnetic influence becomes averaged out; direct detection in frequency domain also permits to get rid of numerical artifacts since advanced numerical filtering is no longer required; if the voltage reversing frequency is different from the setup natural frequencies, ground noise becomes less significant and air motion, being related to the power supply frequency, averages out too. Uncertainties were expected to remain regarding power supply induced EMI.

### **Setup Operation Rationale**

A separate supply of 100 V - AC @ 30 kHz, to three 900 turns parallel mounted toroidal coils and to three parallel mounted 10 nF - 8 mm wide annular capacitors, allows for a total EM momentum (Minkowski’s formulation) around  $5 \text{ E-}11$  Ns (peak), by using BaTiO<sub>3</sub> ceramic dielectrics ( $\epsilon_r \approx 4400$ ). A maximum average thrust around  $0.5 \text{ E-}5$  N should be obtained according to Eq. (20). A reversing frequency of 30 Hz was chosen. Propulsive effects should show up only when the Caps ON – Coils ON condition holds, with a magnitude depending on the set voltage-current phase shift.

## **“Open System” Configuration Results**

The hardware configuration with the device atop the resonant blade and external power supply was adopted for this test series. “Thrust OFF” and Thrust ON” conditions clearly yield different responses in the frequency domain. Phase shift dependence was investigated for PSD peak values at 27 Hz and maxima of the alleged propulsive effect were obtained for a voltage-current phase shift of 90 degrees, as predicted by the proposed formulation. Spreading of the PSD peak values was observed, their source remaining unknown except for fluctuations of ground noise components at the reversing frequency. Nevertheless, a slightly shifted squared sine trend is clearly seen to emerge from data.

## **“Closed System” Configuration Results**

The hardware configuration was modified so the device could be operated in a full “closed system” mode. Both the EMMG and its Power Processing Unit (PPU), including a 12V-1.2 Ah battery, were located and rigidly assembled atop the resonant blade of the sensing fixture. This would allow to assess the influence of external wiring on the previous test series. However, due to the added seismic mass, the thrust stand dynamics was considerably altered and only qualitative analyses could be done. Fully quantitative assessments demand a thoroughly thrust stand characterization, which is currently underway.<sup>20</sup>

Data was processed in the frequency domain, too. To assess the influence of the reversing frequency, tests were carried out at 32 and 38 Hz. Runs of cases “Thrust OFF” and “Coils ON-Caps OFF” behaved as expected, qualitatively similar to the corresponding “Open System” series data. Sharp spectral peaks show up in case “Thrust ON” runs, but, unexpectedly, spectral peaks show up in case “Caps ON-Coils OFF” runs, too, amounting to comparable order of magnitudes regarding “Thrust ON” type peaks. This effect is likely due to the vibratory motion, at the reversing frequency, of a transformer casing in the secondary circuit of the capacitors supply line. Relative phase shift dependence at 32 Hz, taking into account the average peak values under Caps ON – Coils OFF conditions were found to fit a squared-sine law, with maxima at 90 degrees, too.

## **SUSTAINED THRUST EXPERIMENTS - 2**

### **Experimental Setup**

All components were kept without change, except for the EMMG, where the coils and capacitors banks were connected as an LC series circuit, and the PPU which was redesigned to deliver higher power output than the previously used, with an unique output line connected to that LC arrangement.

Power is applied to the EMMG so that  $D$  and  $B$  fields are subjected to harmonic evolution, this time with a fixed  $90^\circ$  phase shift, and a non-zero averaged (sustained) thrust was sought after in virtue of Eq. (20). To take advantage of the sensing device characteristics, the PPU output voltage supply is amplitude modulated following a sine law (instead of a square wave), at a frequency different from the supply frequency, so the seismic setup is set into vibratory motion if the “proposed” formulation is correct. Same considerations as under the previous heading apply regarding the uncertainties due to the expected interferences, although the new modulation procedure was thought to have a beneficial effect by minimizing power supply induced EMI in the PZT measurement line.

### **Modified Setup Operation**

A common supply of 200 V - AC @ 39 kHz, to three 900 turns parallel mounted toroidal coils in series with three parallel mounted 10 nF - 8 mm wide annular capacitors, allows for a total Minkowski’s EM momentum around  $1.E-10$  Ns (peak), by using BaTiO<sub>3</sub> ceramic dielectrics ( $\epsilon_r \approx 4400$ ). An average thrust of  $1.3 E-5$  N should be obtained according to Eq. (20), for  $\varphi = 90$  degrees. Propulsive effects should show up only when the PPU-ON condition holds, with a magnitude depending on the modulation frequency, since the voltage-current phase shift is a built-in property of the LC resonant circuit.

Using of sine modulation of the supply (“carrier”) voltage yields, when Eq. (20) is applied, a modulated average thrust, at the modulation and twice the modulation frequencies, with amplitudes  $1/2$  and  $1/8$ , respectively, of the non-modulated average thrust. This is a thrust model related feature and can be seen as the spectral signature of a sustained EMIM thrust. Since other EM coupling effects can show similar spectra order of magnitude estimates must be done to rule them out.

### **“Open System” Configuration Results**

The device is atop the resonant blade with external power supply. A comparison between “Thrust OFF” and Thrust ON” conditions is shown in Fig. 3. A comparison of “Thrust ON” results with the corresponding simulation results is shown in Fig. 4, where a good agreement is found for the response to the alleged EMIM averaged force at 27 Hz modulation frequency. The response at twice that frequency is underpredicted. Dependence on this parameter was investigated but the useful range stretched between 25 Hz: the minimum modulation frequency outside the noisiest region of the spectrum and 30 Hz: the maximum available modulation frequency. No conclusive results could be obtained since very spread experimental PSD peak values for a given modulation frequency were observed.

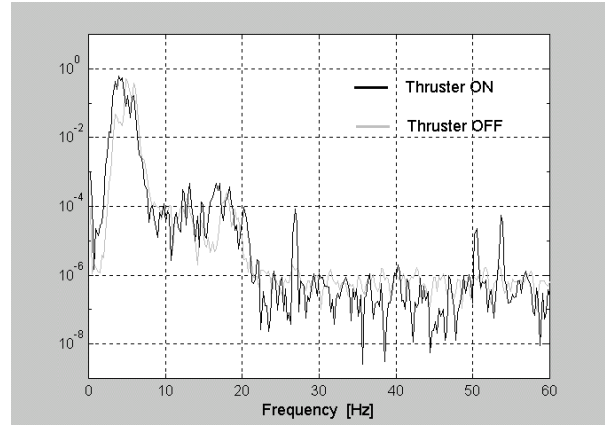


**Fig. 3** Thrust @ 27 Hz effect - PSD [V<sup>2</sup>/Hz].

Spreading of the PSD peak values for a given frequency are thought being related to temperature effect on the capacitors, slight modulation frequency shifts to/from structure natural frequencies or variable battery loading conditions. Their source remains unknown, except as under the previous heading, for fluctuations of ground noise components at the modulation frequency.

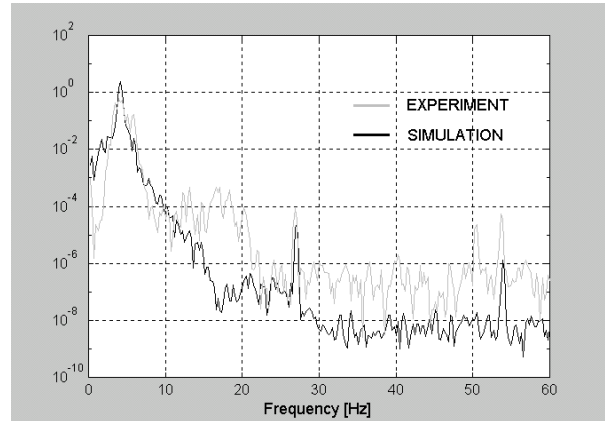


**Fig. 4** “Thrust ON” experimental and simulation results.

### **“Closed System” Configuration Results**

The hardware was configured for full “closed system” mode of operation. Both the EMMG and its redesigned PPU were located and rigidly assembled atop the resonant blade of the sensing fixture. Two 12 V - 1.2 Ah batteries were used instead of a single one. As a result, the total seismic mass is higher than for previous experiments and the first natural frequency of the thrust stand dynamics decreases to 1 Hz. This happens to have a beneficial effect on the vibration isolation characteristics of the whole experimental setup. The residual ground induced motion at the thrust stand base is considerably reduced with respect to former levels; the expected sensing device response to EMIM activation

can now widely overcome the response to ground induced motion. A modulation frequency of 1 Hz was then selected taking advantage of the mechanical amplification factor at resonance. Data was processed in the frequency domain for monitoring purposes, while time domain values were taken as the main experimental results. The PZT conditioned signal was also filtered using sharp low-pass FIR (Finite Impulse Response) filters with a cutoff frequency @ 1.5 Hz. A comparison between “Thrust OFF” (filtered) and Thrust ON” (raw and filtered) response signals is shown in Fig. 5.

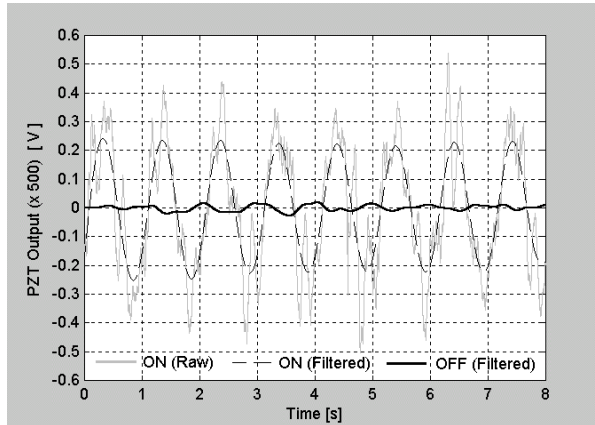


Fig. 5 Sensing device response to EMIM activation.

#### Reassessment of Uncertainties

Although “Open System” sustained thrust experiments were found to get rid of most of the above mentioned interfering effects, “Closed System” versions of those experiments, make appear potential sources of uncertainties (spurious signals), such as<sup>21</sup>

- Electrostatic coupling to surroundings.
- Magnetic coupling to surroundings.
- Self-magnetic couplings.
- Air motion.
- Radiometer effects.
- Ground motion.
- Power supply induced EMI.
- Geomagnetic influence.

which need to be addressed in order to assess their contribution when interpreting the results obtained in time domain in terms of EMIM propulsive effects.

#### Electrostatic Coupling to Surroundings

Alternating electric fields can be significant around the power wires of the EMIM device, where voltage alternates between +200 V and -200 V. Alternating polarization in close-by conductors and insulators can thus be induced. The polarization in insulators can interact directly with the electric fields produced by the power

wiring through the action of induced dipoles on the electric charges that create the field that induce the dipoles. When the voltage and electric charges change sign, the induced voltage will reverse orientation so the interaction can create a force that always act in the same direction on mobile components of the setup, notwithstanding that the electric fields and induced dipoles time-average to zero. Rough but very conservative estimations show that their contribution is two orders of magnitude lower than the observed effect.

Static electric fields due to static electric charges in the surroundings cannot show any effect on static electric charges in the mobile parts of the setup, because PZTs are only sensitive to variable strains (unless special provisions are taken). The situation is in principle different when alternating electric charges in the mobile part are considered. Alternating forces develop that could produce some high frequency component on the PZT output but, having zero time-average, their contribution at the modulation frequency cancels out, too.

#### Magnetic Coupling to Surroundings

Eddy currents in nearby conductors can also be induced by alternating electric fields, which can in turn interact magnetically with currents in the power circuitry of the device. In a way similar to the self-rectifying electrostatic interaction, these forces might induce torques on the sensing device. For this reason, the presence of conductors near that circuitry is minimized and, when present, they are made of non-ferromagnetic materials. Again, rough and very conservative estimations show that their contribution is three orders of magnitude lower than the observed effect.

#### Self-Magnetic Interaction

Self-magnetic interactions in wiring and windings of PPU and EMMG components were also identified as an important potential source of mechanical noise. “Closed System” configuration means that all related current paths must also be closed, belonging then to the whole seismic (or mobile) mass of the thrust stand. If rigid wires and fixations are assumed, no unbalanced force should arise so there would be no contribution to the observed effect. On the contrary, if parts of the circuits are flexible and/or loosely fixed to the casing, inner relative motion will develop under the effect of magnetic forces due to the rest of the circuits. It can be shown that this interaction have a self-rectifying component acting in the same direction on the seismic mass of the setup. Rough but very conservative estimations show that their contribution for flexible wire segments is several orders of magnitude lower than the observed effect, but can amount to about the same order of magnitude for a transformer ferrite casing in the PPU’s secondary circuit.



### Air Motion

Three sources of interference have been considered: a) gradient (thermal, pressure) forced airflow, b) voltage gradient induced airflow (electric wind) and c) sonic wind. Type (a) sources are present even in controlled room environment, although it is highly unlikely that they could bear an oscillatory behavior such as aerodynamic forces act upon the device with the right frequency. Type (b) interferences are known to be proportional to voltage differences between conductors in partially conducting media;<sup>22-24</sup> the voltage being subjected to harmonic evolution, they average out to zero.

Sonic wind arises from nonlinear interaction of air with vibrating parts of the setup being especially apparent when the amplitude of the vibrations of various parts of the device are different.<sup>21</sup> It does not apply here for the whole seismic mass of the setup moves as one, unless vibrating wire segments or casings are considered.

### Radiometer Effects

This effect arises from the differential heating of parts of the device being tested so that reflected molecules of air acquire more momentum in some locations than in others. In this case, heat evolves in the PPU dissipators and in the EMMG coils but these effects can be excluded as a contribution to the observed signal because they do not have the right signature. As a temperature induced effect, given the involved heat capacities, is a smoothly cumulative one so it cannot account for 1 Hz vibration frequencies.

### Ground Motion

Ground motion contributes to the observed signal by means of the resulting inertial forces acting upon the sensing device seismic mass. This device being essentially a fourth order mechanical filter, that contribution consists of a colored noise mostly centered around the two main structure vibration modes, as can be seen in Fig. 4 for the “Open System” setup configuration: 4.5 and 18 Hz. The 50 Hz component is instead of electrical origin corresponding to the AC network frequency going into the measurement lines by imperfect shielding. As mentioned above, the ground motion noise @ 1Hz is considerably lower for the actual “Closed System” setup than for any of the previously used setups. Typical levels are shown in Fig. 6 where raw and numerically filtered data are plotted vs. time, for the thruster in OFF condition. These levels correspond to quiet acoustic-seismic environment (no walking around, nearby city traffic, wind, etc.). Several runs under such environmental constraints produce, after filtering, an enlarged set of data with zero mean and  $\sigma = 0.007$  V. The ground motion influence @ 1 Hz can thus conservatively be estimated to lie within the  $\pm 0.02$  V band.

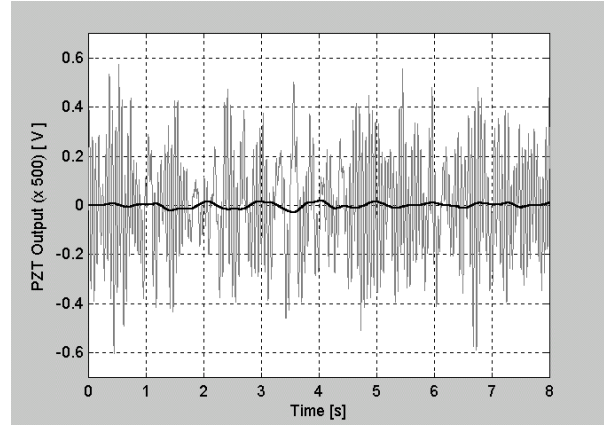


Fig. 6 “Thrust OFF” raw and filtered experimental data.

### Power Supply Induced EMI

Power supply-induced electromagnetic interference (EMI) on the measurement channels, sharing the same spectral signature with the pursued effect, has been deemed an issue in former test series, where no attempt was done of assessing its influence on the observed results. The obvious 50 Hz EMI example has already been called forth and similar interference was expected to occur as related to modulated thruster input power.

The thrust stand has a built-in feature allowing to fasten the normally free upper end of the resonant blade for safety and transport purposes. Transverse displacements can thus be limited, not rotations. If these “brakes” are used during “Thruster ON” runs, when the modulated power is fully in action, a drastic reduction of the signal is observed, as compared with the same “Thruster ON” runs when the “brakes” are not applied. Results shown in Fig. 7 are considered as a practical proof that this effect amount to less than 5% of the observed signal.

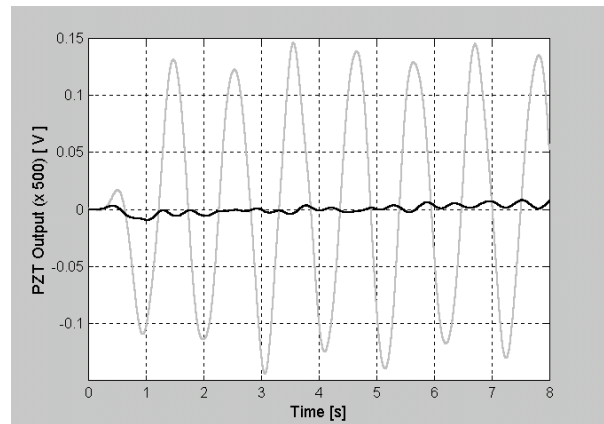


Fig. 7 “Thruster ON” sensing device response for “free” (gray) and “fastened” (black) blade upper end.



Geomagnetic Influence

By modulating the voltage supply at a frequency different from the “carrier” frequency, so the seismic setup is excited at the modulation frequency if the “proposed” formulation is correct, the geomagnetic influence becomes averaged out in the “Open System” setup configuration; the same cannot be said regarding “Closed System” configurations. In fact, in these cases, the force producing device is self-contained, with all its components, including batteries, sitting in the suspended frame of the sensing fixture. Since the PPU output voltage is required to be modulated, current from the batteries will accordingly be modulated around an almost constant value without sign reversing. As a result, a coupling with the Earth’s magnetic field should be expected and since there are no external parts of the circuit, the interaction develops through closed current loops which applies torques on the fixture.

The PZT based sensing mechanism is also sensitive to torques. They can be mistaken as forces acting upon the free end of the cantilever beam, if some discriminating procedure is not applied. An important feature to be taken into account is that the sensing mechanism is only sensitive to the component of the torque which lies transversally in the plane of the blade. This means that the significant components of the geomagnetic field with respect to the blade are the vertical (longitudinal) and the perpendicular ones; they are related to the vertical (parallel to the blade’s plane) and the horizontal projections of the current loop, respectively .

It is easy to see that, for a given PPU orientation with respect to the blade, the torque due to the vertical projection is a built-in property of the setup, not depending on the thrust stand azimuth angle. Instead, the torque due to the horizontal projection does show a cosine dependence on that angle. Therefore, by performing tests at various azimuth angles, the influence of that torque contribution can be complete and quantitatively assessed. In order to investigate other spurious influences as mentioned above, tests were devised with the PPU operating at nominal conditions, though powering an EMMG electrical emulator, instead of the thruster itself. The emulator consists of a RLC circuit electrically equivalent to the EMMG (same input impedance) and is connected to the PPU by means of feeds in practically the same geometrical configuration. A ground reference frame was also adopted with the horizontal axes parallel to the room walls:  $X_G$  axis pointing 10 deg. East of magnetic North;  $Y_G$  axis pointing eastward, and  $Z_G$  axis pointing to ground. A local reference frame was ascribed to the thrust stand:  $X_T$  axis along the EMMG longitudinal axis;  $Z_T$  axis along the longitudinal axis of the blade, pointing toward its clamped end, and  $Y_T$  forming a direct orthogonal frame with the other

two axes. Naming  $\psi$  the angle between  $X_T$  and  $X_G$ , mean amplitudes and  $1\sigma$  errors obtained for different thrust stand orientations are shown in Table 1.

**Table 1** PPU ON – EMMG OFF sensing device response

$\psi$			
0 deg	90 deg	180 deg	270 deg
0.17 ±0.009	0.136 ±0.006	0.11 ±0.005	0.134 ±0.007

The response mean values closely agree with a  $\cos \psi$  dependence but in spite of lacking intermediate values, two important features arise from these figures: 1) They do not vanish at 90 and 270 deg, as one should expect were the geomagnetic field horizontal (perpendicular to the blade) component the only acting effect. There is a 0.14 V offset which, in principle, could be ascribed to the vertical component. 2) The peak to peak excursion is around 0.06 V so the contribution of the horizontal component cannot be higher than 0.03 V. To settle the question the PPU orientation was reverted with respect to the EMMG and tests were performed, again using the EMMG emulator. The results are shown in Table 2.

**Table 2** PPU ON – EMMG OFF sensing device response with reverted PPU orientation

$\psi$			
0 deg	90 deg	180 deg	270 deg
0.11 ±0.006	0.053 ±0.004	N/A	N/A

Combining the results of Tables 1 and 2, consistent values for the horizontal and vertical component contributions can be found provided an additional, non-geomagnetic, effect is taken into account. Both the horizontal and vertical components contribute to around 0.03 V, while the residual contribution is around 0.1V.

It is considered that the observed residual effect is largely due to inner motions related to a transformer ferrite made casing in the PPU’s secondary circuit, with minor contribution from eventual electrostatic and magnetic couplings to surroundings, self-magnetic interactions involving loose wiring and, within a negligible extent, to air motion. These residual effects are also expected to appear during testing under “PPU ON-EMMG ON” conditions.

### EMIM Thrusting Results

Tests with activation of the EMMG were performed at various azimuth angles as under the previous sub-heading, keeping the nominal PPU orientation. The obtained results are shown in Table 3, as mean and  $1\sigma$  errors values.

**Table 3** PPU ON – EMMG ON sensing device response

<hr/> <hr/>				
		$\psi$		
0 deg	90 deg		180 deg	270 deg
<hr/>				
0.21 $\pm$ 0.01	0.26 $\pm$ 0.01		0.28 $\pm$ 0.008	N/A
<hr/> <hr/>				

The response mean values fairly agree with a  $\cos \psi$  law but they are considerably higher than those obtained during the emulator tests. There is indeed a new effect which adds up to those previously investigated. Since amplitudes of vibration are involved in this study, by comparing the results of Table 1 and 3, it seems that this new effect has either a  $\cos \psi$  dependence w.r.t. the geomagnetic field or is nearly constant ( $0.39 \pm 0.02$  V). In both situations the 0.1 V residual effect simply cancels out if induced by PPU circuitry and components. A constant value is entirely consistent with thrust being produced by the EMMG, depending only on the power delivered by the PPU, which was kept fixed at 200 V on EMMG's capacitors and coils. The claim here is that the new observed results correspond to a genuine electromagnetic inertia manipulation propulsive effect. Thrust stand simulations according to a model presented elsewhere,<sup>20</sup> yield a sensing device mean response amplitude of 0.38 V after 20 seconds of EMMG activation, including micro-seismic (ground motion) excitation which accounts for  $\pm 0.01$  V peak values  $1\sigma$  dispersion.

### CONCLUSIONS

The possibility of achieving thrust without reaction mass or beamed power, by means of EM inertia manipulation, has been reviewed. Experimental confirmation of this theoretical concept was sought after and instrumented around a so called EMIM force-producing device. Tests performed during an exploratory phase produced results, which after intensive data processing gave indirect evidence of matter-electro-magnetic field momentum exchange, as predicted by Minkowski's formalism; direct detection of the sought effect could not be achieved due to interfering effects leading to very low S/N ratios. Sustained thrust experiments based

on an alternative formulation of the EM force densities were devised and performed aiming at getting rid of most of the identified spurious effects, yielding sharp and clear evidence of force-producing effects as predicted by that formulation, albeit in contradiction with null results predicted by the "standard" formulation.

New experimental results where increased power and sine modulated voltage at a frequency close to the fundamental frequency of the sensing fixture have been applied, allowed to confirm previous results with the alleged propulsive effect showing up well over the ground induced noise. Self-magnetic interactions in wiring and windings of the PPU's components having been identified as an important source of mechanical noise, their influence has been estimated and experimentally assessed as being a minor part of the observed effect. Furthermore, power supply induced EMI on the measurement channels, sharing the same spectral signature with the pursued effect, if present was found to contribute to less than 5% of the observed effect. Other sources of uncertainties have been identified and deemed negligible for all practical purposes. Some uncertainties remain as related to PZT's compression mode sensitivity to inner motions which might behave differently in thrusting and emulator tests, and unidentified inner motions which might not eventually show up during EMMG emulator tests. The former are expected to be overcome by means of Laser Doppler Vibrometry techniques while the latter would require a complete redesign of the thruster. Definite answers will have to wait until in-orbit testing could be performed, simultaneously getting rid of all kind of interferences. Present and previous thrust results seem to closely fit theoretical predictions from a conjectural approach which, in turn, has been found consistent with including the polarization currents in Lorentz force calculations. If this "anomalous" thrusting effect still persists, propellantless propulsion would have been achieved but additional theoretical work will be needed for full understanding of the underlying physical principles.

### ACKNOWLEDGMENTS

The author wishes to thank the U.S. Air Force Research Laboratory for supporting the presentation of this work under its Windows-on-Science Program, Grant Nr. FA8655-03-1-2A21, and to NASA BPP Project for procuring that help. Support from the Argentine National Agency for the Advancement of Science and Technology (ANPCyT), Grant FONCyT - PICT-99-10-07107, and "Instituto Universitario Aeronautico" of Cordoba, Argentina, are also gratefully acknowledged.

## REFERENCES

- <sup>1</sup> Clarke, A. C., "Profiles of the Future," *Beyond the Gravity*, Pan Books Ltd., London, 1962, pp. 52-64.
- <sup>2</sup> Brito, H. H., "A Propulsion-Mass Tensor Coupling in Relativistic Rockets Motion," *Proceedings of the Space Technology Applications International Forum (STAIF-98)*, Part Three, Institute for Space and Nuclear Power Studies, Albuquerque, NM, 1998, pp. 1509-1515.
- <sup>3</sup> Brevik, I., "Definition of some Energy-Momentum Tensors," *Experiments in Phenomenological Electrodynamics and the Electromagnetic Energy-Momentum Tensor*, PHYSICS REPORT (Review Section of Physics Letters) Vol. 52, No. 3, North Holland Publishing Co., Amsterdam, 1979, p. 139.
- <sup>4</sup> Antoci, S., Mihich, L., "A forgotten argument by Gordon uniquely selects Abraham's tensor as the energy-momentum tensor for the electromagnetic field in homogeneous, isotropic matter," *Nuovo Cimento B*, Vol. 112B, 1997, pp. 991-1007.
- <sup>5</sup> Johnson, F. S., Cragin, B. L., Hodges, R. R., "Electromagnetic momentum density and the Poynting vector in static fields," *American Jnl. of Physics*, Vol. 62, 1994, pp. 33-41.
- <sup>6</sup> Jackson, J. D., "Time-Varying Fields, Maxwell's Equations, Conservation Laws," *Classical Electrodynamics*, 2<sup>nd</sup> Ed., John Wiley & Sons, Inc., New York, 1962, pp. 169-202.
- <sup>7</sup> Portis, A. M., "Fuentes del campo electromagnético III - Cantidad de movimiento del campo," *Campos Electromagnéticos*, Sp. ed., Vol. 2, Ed. Reverté, Barcelona, 1985, pp. 469-472.
- <sup>8</sup> Eu, B. C., "Statistical foundation of the Minkowski tensor for ponderable media," *Phys. Review A*, Vol. 33, 1986, pp. 4121-4131.
- <sup>9</sup> Brito, H. H., "Propellantless Propulsion by Electromagnetic Inertia Manipulation: Theory and Experiment," *AIP Conference Proceedings 458*, American Institute of Physics, New York, 1999, pp. 994-1004.
- <sup>10</sup> Brito, H. H., "Research on Achieving Thrust by EM Inertia Manipulation," AIAA Paper 2001-3656, Salt Lake City, Utah, July 2001.
- <sup>11</sup> Brito, H. H., "Experimental Status of Thrusting by Electromagnetic Inertia Manipulation," Paper IAF-01-S.6.02, 52<sup>nd</sup>. International Astronautical Congress, Toulouse, France, Oct. 2001.
- <sup>12</sup> Lai, H. M., "Electromagnetic momentum in static fields and the Abraham-Minkowski controversy," *American Jnl. of Physics*, Vol. 48, 1980, pp. 658-659.
- <sup>13</sup> Brevik, I., "Comment on "Electromagnetic Momentum in Static Fields and the Abraham-Minkowski Controversy"," *Physics Letters*, Vol. 88 A, 1982, pp. 335-338.
- <sup>14</sup> Lai, H. M., "Reply to "Comment on 'Electromagnetic Momentum in Static Fields and the Abraham-Minkowski Controversy'"", *Physics Letters*, Vol. 100 A, 1984, p. 177.
- <sup>15</sup> Furry, W. H., "Examples of Momentum Distributions in the Electromagnetic Field and in Matter," *American Jnl. of Physics*, Vol. 37, 1969, pp. 621-636.
- <sup>16</sup> Brito, H. H., "Tensor Mass – Isomassic Solution to the Space Propulsion Problem," submitted to the National Academy of Sciences (Argentina), Cordoba, Sept. 1982.
- <sup>17</sup> Will, C. M., "The Theoretical Tools of Experimental Gravitation," *Experimental Gravitation*, Academic Press Inc., New York, 1973, pp. 71-72.
- <sup>18</sup> Walker, G. B., Walker, G., "Mechanical forces in a dielectric due to electromagnetic fields," *Canadian Jnl. of Physic*, Vol. 55, 1977, pp. 2121-2127.
- <sup>19</sup> Forward, R. L., "Picostrain measurements with piezoelectric transducers," *Jnl. of Applied Physics*, Vol. 51, 1980, pp. 5601-5603.
- <sup>20</sup> Brito, H. H., Garay, R., Duelli, R., Maglione, S., "A Compact, Low-Cost Test Stand for PPT Impulse Bit Measurements," AIAA Paper 2000-3545, July 2000.
- <sup>21</sup> Woodward, J. F., Mahood, T. L., "Mach's Principle, Mass Fluctuations and Rapid Spacetime Transport," *AIP Conference Proceedings 504*, American Institute of Physics, New York, 2000, pp. 1018-1025.
- <sup>22</sup> Cheng, S. I., "Glow Discharge as an Advanced Propulsion Device," *ARS Journal*, Vol.12, 1962, pp. 1910-1916.
- <sup>23</sup> Loeb, L. B., "Electric Coronas," *Their Basic Physical Mechanisms*, University of California Press, 1965.
- <sup>24</sup> Christensen, E. A., Moller, P. S., "Ion-Neutral Propulsion in Atmospheric Media," *AIAA Journal*, Vol.1.5, No. 10, 1967, pp. 1768-1773.